

Supporting Information for:

**Kinetic Analysis of Photoelectrochemical Water Oxidation
by Mesostructured Co-Pi/ α -Fe₂O₃ Photoanodes**

Gerard M. Carroll and Daniel R. Gamelin*

Department of Chemistry, University of Washington, Seattle, WA 98195-1700

*Email: gamelin@chem.washington.edu

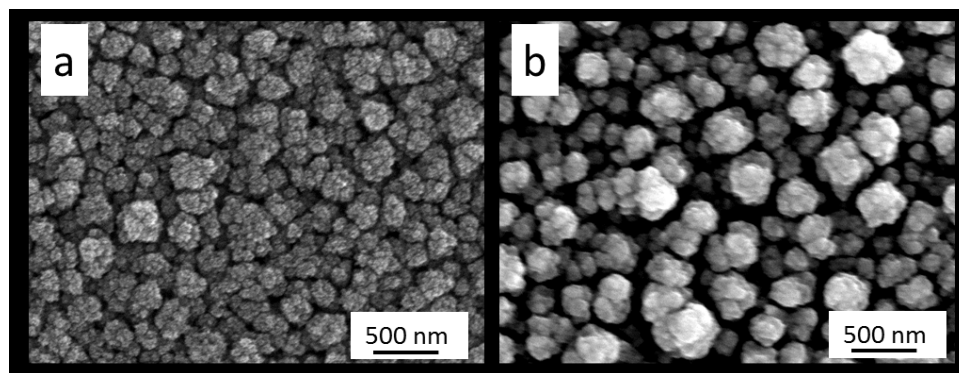


Figure S1. SEM images of (a) bare α -Fe₂O₃ and (b) 24.6nm thick Co-Pi coated α -Fe₂O₃

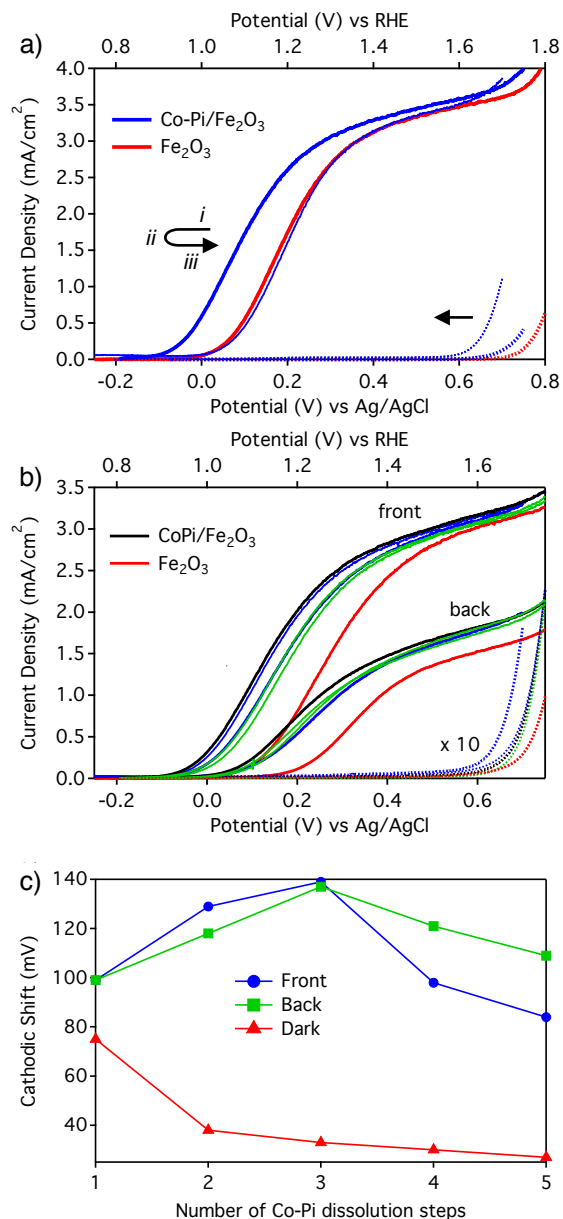


Figure S2. (a) $J-V$ curves of an $\alpha\text{-Fe}_2\text{O}_3$ photoanode (*i*, red) and of the same photoanode modified with thin (*ii*, dark blue) and thick (*iii*, light blue) Co-Pi layers, measured in 1 M NaOH under 1 sun AM 1.5 simulated sunlight (solid) and in the dark (dotted). (b) $J-V$ curves for an $\alpha\text{-Fe}_2\text{O}_3$ photoanode measured before (red) and after (light blue) photo-assisted electrodeposition of a thick layer of Co-Pi. Additional curves were measured after various durations of Co-Pi dissolution (ending with light green). (c) Cathodic shifts of the onset potentials from panel (b), measured over the course of Co-Pi dissolution in the dark (red), under front-side illumination (blue), and under backside illumination (green). Measurements were made in 1 M NaOH at a scan rate of 10 mV/s. Data courtesy of Dianne Zhong (UW).

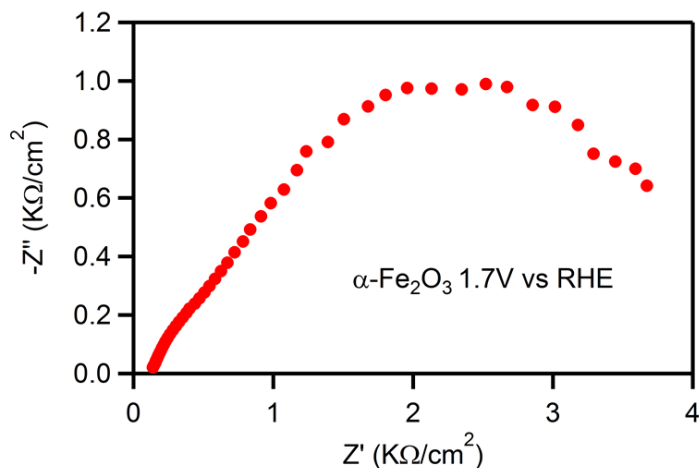


Figure S3. Nyquist plot of the highest potential measured in the impedance analysis of a bare $\alpha\text{-Fe}_2\text{O}_3$ photoanode.

In planar $\alpha\text{-Fe}_2\text{O}_3$ films, the capacitive feature of the low-frequency semicircle disappears at potentials more positive than +1.5 V vs RHE, attributable to fast (non-rate-limiting) hole transfer from surface states.¹⁻⁴ Here, the capacitive feature at low frequencies is visible up to $\sim +1.7$ V vs RHE, suggesting that hole transfer to water remains rate limiting throughout the voltammetric window of interest.

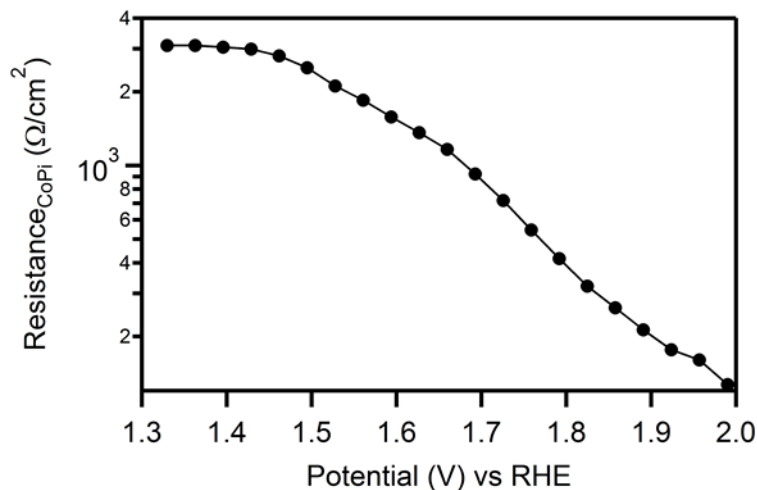


Figure S4. Charge-transfer resistance ($R_{\text{Co-Pi}}$) values of Co-Pi/FTO anodes, measured in 0.1M KPi, pH 8. The solid line is a guide to the eye.

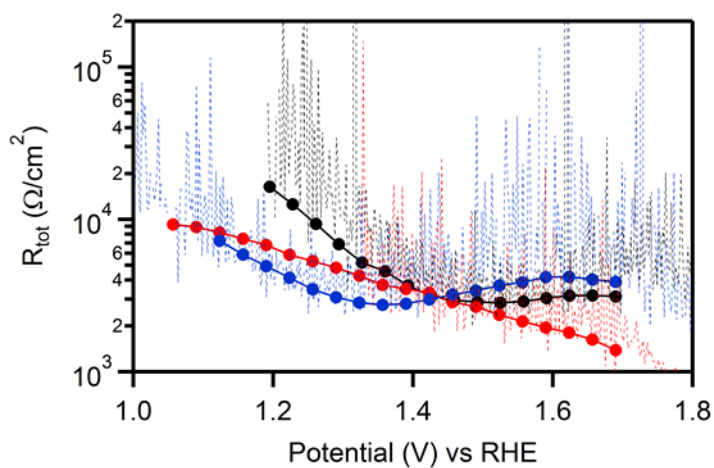


Figure S5. Differential-resistance (dV/dI) data (dashed lines) and R_{TOT} data (closed circles) for bare α - Fe_2O_3 (black), ~ 2.3 nm Co-Pi/ α - Fe_2O_3 (blue), and ~ 24.6 nm Co-Pi/ α - Fe_2O_3 (red) photoanodes, plotted vs applied potential. Experimental details are described in the main text.

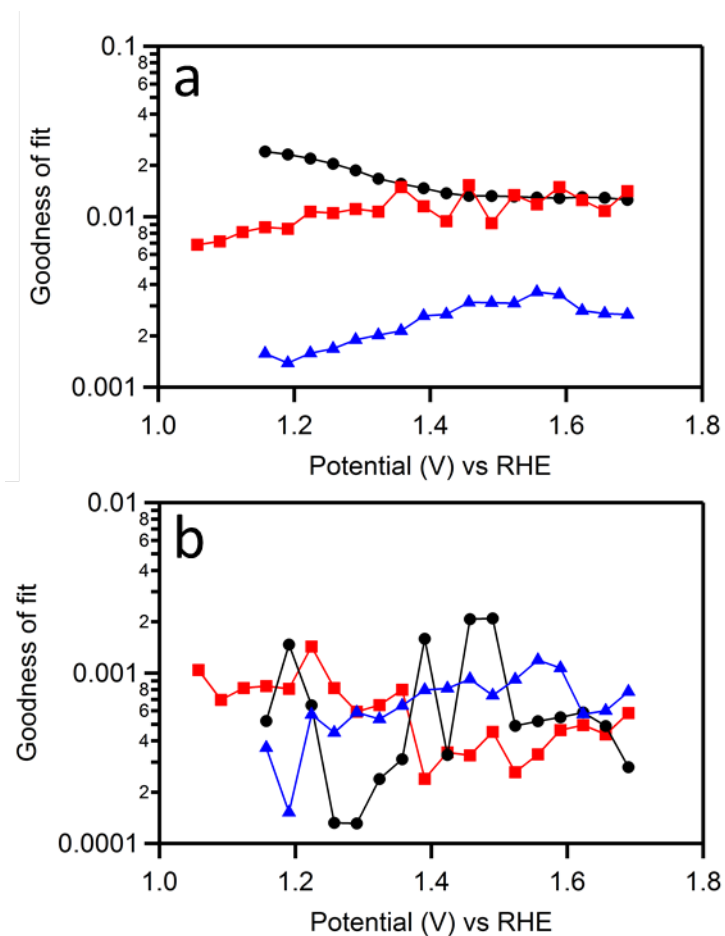


Figure S6. Goodness-of-fit values between the experimental EIS data and the model for bare $\alpha\text{-Fe}_2\text{O}_3$ (black circles), optimized Co-Pi/ $\alpha\text{-Fe}_2\text{O}_3$ (blue triangles), and bottlenecked Co-Pi/ $\alpha\text{-Fe}_2\text{O}_3$ (red squares) photoanodes. (a) Values obtained from modeling with a standard capacitor model. (b) Values obtained from a constant phase element model. Values between 0.001 and 0.01 correspond to between ~ 3 and 10% difference between the data and the fit.

Capacitance values from models containing a constant phase element (CPE) were obtained using equation S1, where α is an empirical value obtained from the EIS fit and ω_{\max} is the frequency at the maximum phase angle.

$$Capacitance = CPE \times (\omega_{\max})^{\alpha-1} \quad (S1)$$

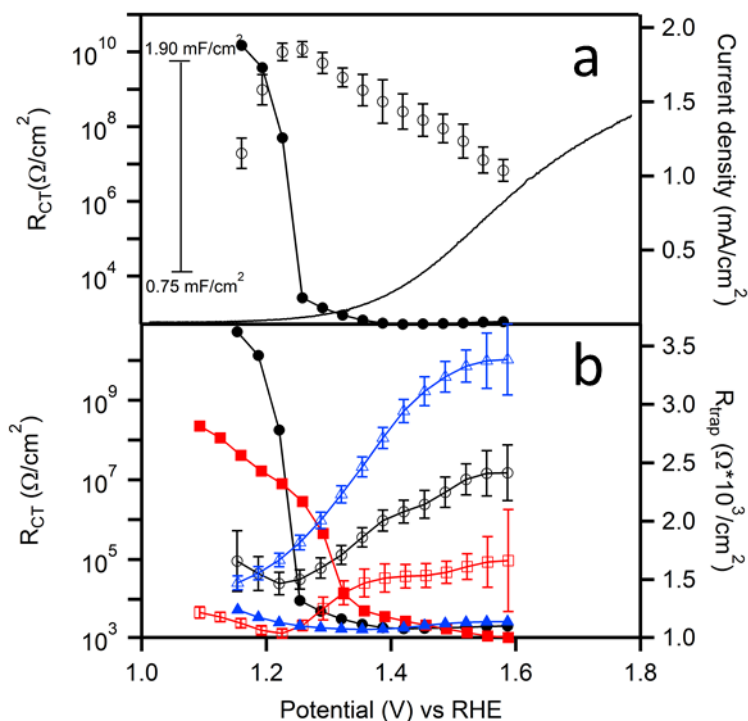


Figure S7. (a) R_{CT} SS (closed circles), C_{SS} (open circles), and J - V (solid line) data obtained for a bare $\alpha\text{-Fe}_2\text{O}_3$ photoanode. These R_{CT} SS and C_{SS} data were obtained from the PEIS data by fitting using a constant phase element. The linear inset scale bar refers to the C_{SS} data. Error bars correspond to uncertainties from the impedance fitting. **(b)** R_{CT} (closed shapes) and R_{trap} (open shapes) data for the same $\alpha\text{-Fe}_2\text{O}_3$ photoanode measured with 0 (black circles), ~ 2.3 (blue triangles), and ~ 24.5 nm Co-Pi (red squares) surface coverage. These data are presented for comparison with the data in Figure 3 of the main text.

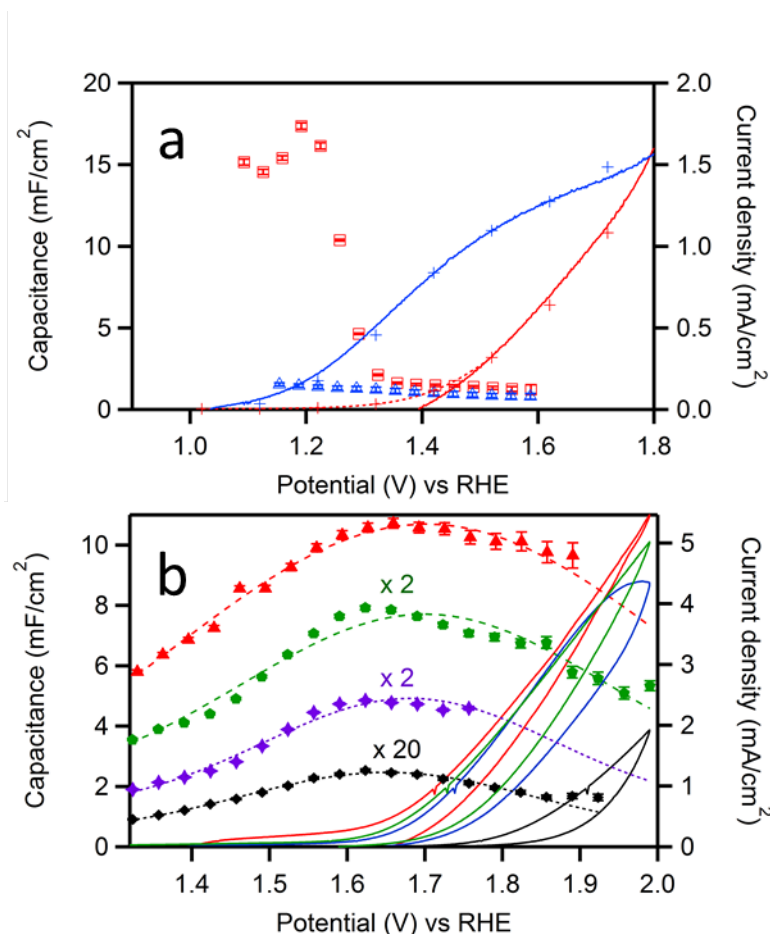


Figure S8. (a) $C_{SS\ Co-Pi}$ (open shape) and $J-V$ (solid line) data measured for the same α - Fe_2O_3 photoanode with ~ 2.3 nm (blue triangle) and ~ 24.5 nm (red square) thick Co-Pi on its surface. Measurements were collected under AM 1.5 illumination from the back side in 0.1 M KPi at pH 8 and fit using a constant phase element. The hash mark symbols on the $J-V$ curves show steady-state current densities. (b) C_{TOT} (closed shapes), and $J-V$ (solid lines) data measured at 10 mV/s scan rate for the same FTO anode with ~ 1.2 nm (black diamond), ~ 24.5 nm (purple star), ~ 46.8 nm (green pentagon), and ~ 490 nm (red triangle) Co-Pi thickness on the surface. The dashed lines are guides to the eye.

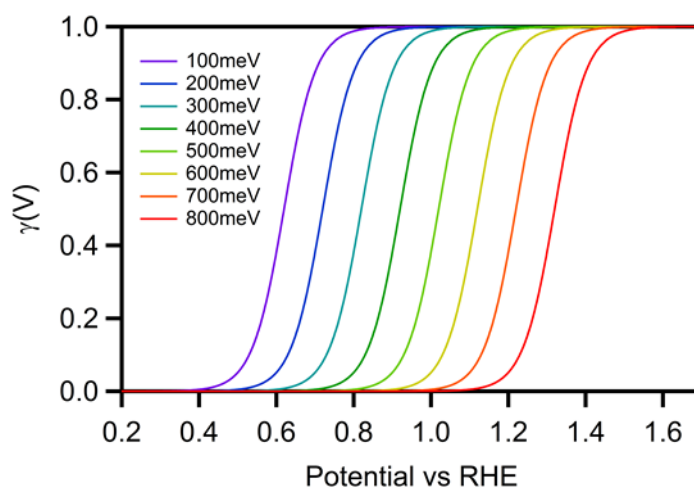


Figure S9. Calculated values of $\gamma(V)$ as a function of applied potential. Electron trap energies between 100 and 800 meV more negative than the equilibrium Fermi level of the electrode are shown.

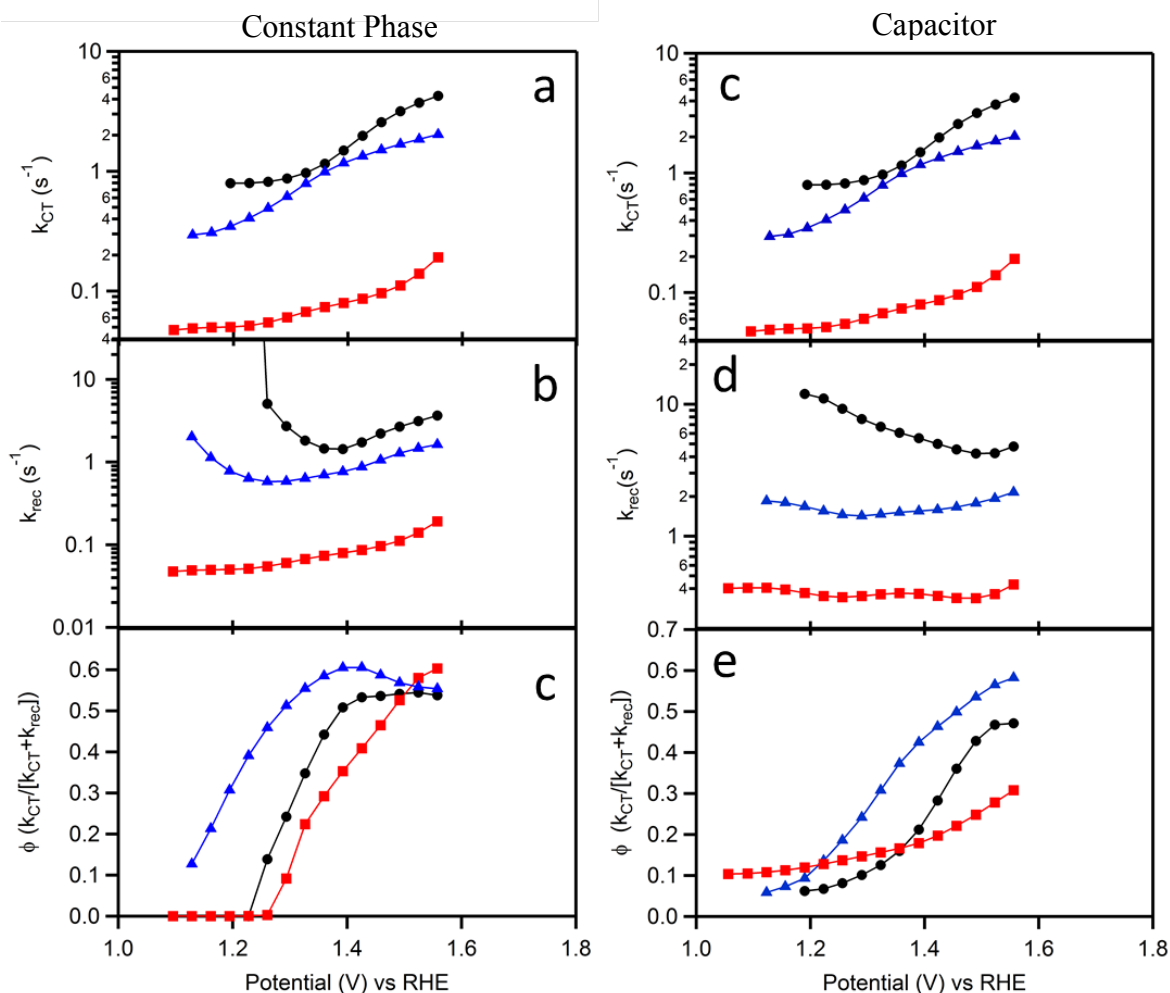


Figure S10. (a,c) Charge-transfer rate constants, (b,d) recombination rate constants, and (c,e) water-oxidation quantum efficiency plotted vs applied potential for bare α -Fe₂O₃ (black circles), 2.3 nm Co-Pi/ α -Fe₂O₃ (blue triangles), and 24.5 nm Co-Pi/ α -Fe₂O₃ (red squares) photoanodes. Panels a, b, and c plot values obtained from fitting impedance data with a constant phase element for comparison with panels d, e, and f, which plot the results from Figure 5 in the main text.

- (1) Klahr, B.; Gimenez, S.; Fabregat-Santiago, F.; Bisquert, J.; Hamann, T. W. *Energy Environ. Sci.* **2012**, *5*, 7626.
- (2) Klahr, B.; Hamann, T. *J. Phys. Chem. C* **2014**, *118*, 10393.
- (3) Klahr, B. M.; Hamann, T. W. *J. Phys. Chem. C* **2011**, *115*, 8393.
- (4) Bertoluzzi, L.; Bisquert, J. *J. Phys. Chem. Lett.* **2012**, *3*, 2517.